PHYSICAL REVIEW B **79**, 201404(R) (2009)

Crossover from quantum to Boltzmann transport in graphene

Shaffique Adam,[1] Piet W. Brouwer,[2] and S. Das Sarma[1]
[1]*Condensed Matter Theory Center, Department of Physics, University of Maryland, College Park, Maryland 20742-4111, USA*
[2]*Laboratory of Atomic and Solid State Physics, Cornell University, Ithaca, New York 14853-2501, USA*
(Received 6 May 2009; published 22 May 2009)

We compare a fully quantum-mechanical numerical calculation of the conductivity of graphene to the semiclassical Boltzmann theory. Considering a disorder potential that is smooth on the scale of the lattice spacing, we find quantitative agreement between the two approaches away from the Dirac point. At the Dirac point the two theories are incompatible at weak disorder, although they may be compatible for strong disorder. Our numerical calculations provide a quantitative description of the full crossover between the quantum and semiclassical graphene transport regimes.

DOI: 10.1103/PhysRevB.79.201404 PACS number(s): 73.23.−b, 72.10.−d, 73.40.−c, 81.05.Uw

Arguably, one of the most intriguing properties of graphene transport is the nonvanishing "minimum conductivity" at the Dirac point. The carrier density n in these single monatomic sheets of carbon can be continuously tuned from electronlike carriers for large positive gate bias to holelike carriers for negative bias.[1] The physics close to zero carrier density (also called the intrinsic or Dirac region) is now understood to be dominated by the inhomogeneous situation where the local potential fluctuates around zero, breaking the landscape into puddles of electrons and holes.[2] In the literature, two separate pictures have emerged to understand the value of this minimum conductivity. The first picture expands around the universal value for the minimum conductivity $\sigma_{\min}=4e^2/(\pi h)$ for clean graphene[3] and argues that the presence of potential fluctuations smooth on the scale of the graphene lattice spacing *increases* the conductivity through quantum interference effects.[4–7] The second picture extrapolates to the Dirac region from the high-density limit, where the conductivity for charged impurity scattering can be calculated using the semiclassical Boltzmann theory. This approach has been further refined near the Dirac point by positing that the system acquires an effective carrier density n^* calculated from the rms density fluctuations (associated with the electron-hole puddles) about the Dirac point caused by the same impurities that are responsible for the scattering of carriers at high density.[8] These two conceptually different approaches lead to strikingly different predictions for the conductivity at the Dirac point: The Boltzmann transport theory for Coulomb disorder predicts that increasing disorder *decreases* the conductivity, whereas the weak antilocalization picture has a conductivity that *increases* with increasing disorder strength. Given their vastly different starting points, it is not surprising that the two approaches disagree.

A direct comparison between the two approaches has not been possible mainly because the published predictions of the Boltzmann approach include screening of the Coulomb disorder potential, whereas the fully quantum-mechanical numerical calculations are for a noninteracting model using Gaussian disorder. Notwithstanding the fact that screening and Coulomb scattering play crucial roles in transport of real electrons through real graphene,[9] the important question of the comparison between quantum and Boltzmann theories has remained unanswered, even for the Gaussian disorder case. It is the goal of this work to provide such a comparison, thereby establishing the bridge between these two widely used complementary theoretical approaches to transport in graphene.

In what follows we consider noninteracting electrons at zero temperature in a Gaussian correlated disorder potential that varies smoothly on the scale of the graphene lattice spacing. This situation is described by the effective Hamiltonian $\mathcal{H}=\sigma\cdot\mathbf{p}+U(\mathbf{r})$, where v is the Fermi velocity, $\mathbf{p}$ is the (two-dimensional) momentum, and $U(\mathbf{r})$ is a random Gaussian potential with correlation function,

$$\langle U(\mathbf{r})U(\mathbf{r}')\rangle = K_0\frac{(\hbar v)^2}{2\pi\xi^2}e^{-|\mathbf{r}-\mathbf{r}'|^2/2\xi^2}, \tag{1}$$

where ξ is the correlation length and K_0 is a dimensionless parameter that parametrizes its magnitude. Typical experimental conditions correspond to K_0 between 1 and 3.[10,11] We numerically solve the full quantum problem for a sample of finite size $L\gg\xi$, starting from intrinsic graphene where quantum coherence effects dominate to high doping where quantum effects are a small correction to the conductivity.[12] We have compared the numerical results to predictions of the Boltzmann theory, its self-consistent modification of Ref. 8, and weak antilocalization corrections for a range of disorder strength K_0 and carrier densities n.

Our main conclusions, to be supported by the material below, are: (i) away from the Dirac point, both the Boltzmann theory and the full quantum solution agree to leading order, $\sigma\propto n^{3/2}$, with deviations only in terms of order $n^{1/2}$ and smaller. This validates the assumptions of both theories, i.e., the Born approximation for the Boltzmann approach and use of a finite sample size in the numerical approach. (ii) At the Dirac point, the quantum conductivity increases with increasing disorder strength K_0; for $K_0\gg 1$ the increase is compatible with the self-consistent Boltzmann theory. (iii) As a function of carrier density, the quantum conductivity, but not the Boltzmann conductivity, shows a sharp reduction at the Dirac point, which is most pronounced for $K_0\sim 1$; the conductivity becomes proportional to $1/K_0$ away from the Dirac point; and (iv) the numerical quantum results are consistent with $d\sigma/d\ln L=4e^2/\pi h$ for $\sigma\gtrsim 4e^2/h$, *irrespective of the carrier density* n, consistent with the weak antilocalization

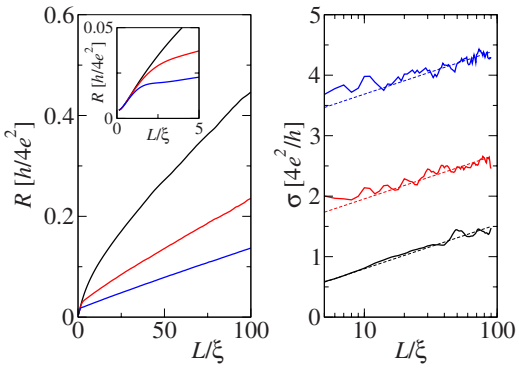

FIG. 1. (Color online) Resistance $R=1/G$ (left) and conductivity σ obtained using Eq. (4) (right), as a function of sample length L. The three curves shown are for $W/\xi=200$, $K_0=2$, and $\pi n\xi^2=0$, 0.25, and 1 [from top to bottom (bottom to top) in left (right) panel]. Dashed lines in the right panel show $d\sigma/d\ln L=4e^2/\pi h$. The inset in the left panel shows the crossover to diffusive transport ($L\gg\xi$).

theory. Our numerical calculations provide a quantitative description of the full crossover between the quantum and semiclassical transport regimes for which no analytical theory is available.

The Boltzmann conductivity corresponding to the model of Eq. (1) is calculated using the relation $\sigma=e^2\nu v_F^2\tau/\hbar$, where $\nu=4k_F/\pi\hbar v_F$ is the density of states and the elastic relaxation time τ is given by

$$\frac{1}{\tau}=\int\frac{d\mathbf{q}d\mathbf{r}}{4\pi\hbar}(1-\cos^2\theta_{\mathbf{q}})\delta(k_F-q)\langle U(0)U(\mathbf{r})\rangle e^{i\mathbf{q}\cdot\mathbf{r}},$$

where $\theta_{\mathbf{q}}$ parametrizes the direction of $\mathbf{q}$ so that

$$\sigma_B=\frac{4e^2}{h}\frac{\pi n\xi^2 e^{\pi n\xi^2}}{K_0 I_1(\pi n\xi^2)}=\frac{2\sqrt{\pi}e^2}{K_0 h}[(2\pi n\xi^2)^{3/2}+\mathcal{O}(n\xi^2)^{1/2}], \tag{2}$$

with the carrier density $n=k_F^2/\pi$. The leading term for large density can also be obtained considering the classical diffusion of a particle undergoing small-angle deflections from the random potential U.[13] The weak antilocalization correction to the conductivity is[4]

$$\delta\sigma(L,\ell)=\frac{4e^2}{\pi h}\ln(L/\ell), \tag{3}$$

where ℓ is the transport mean-free path. In the Boltzmann theory, ℓ can be obtained from the relation $\sigma_B=2(e^2/h)k_F\ell$. A self-consistent modification of the Boltzmann theory was proposed in Ref. 8 in order to describe transport near the Dirac point $n=0$. For our Gaussian model of disorder, this modification involves replacing the carrier density by a "self-consistent" carrier density $n^*=\pi^{-1}(\varepsilon_F^*/\hbar v_F)^2$, where $\varepsilon_F^{*2}=\langle(\varepsilon_F+U)^2\rangle$.[14] We then find $n^*=|n|+K_0/2\pi^2\xi^2$, and the self-consistent prediction for the conductivity is given by Eq. (2) above with n replaced by the self-consistent density n^*.

In the numerical calculation we consider a graphene strip of dimensions $L\times W$ with W, $L\gg\xi$, connected to highly doped graphene regions on both ends. Following the method described in Ref. 5, we calculate the conductance G of the graphene strip. The conductivity σ is then obtained using the relation

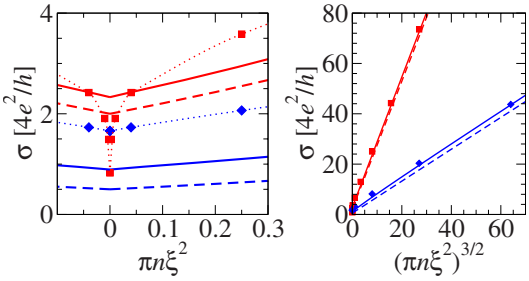

FIG. 2. (Color online) Conductivity σ versus carrier density n. The left panel shows the low-density behavior near the Dirac point; the right panel shows the high-density behavior. Data points are from numerical simulation with $K_0=1$ (squares) and $K_0=4$ (diamonds) with dotted lines in the left panel as a guide to the eyes. The dashed curves show the predictions of the Boltzmann theory, and the solid lines show the self-consistent Boltzmann result.

$$\sigma=\left[W\frac{dR}{dL}\right]^{-1},\quad R=1/G. \tag{4}$$

We verify that our results do not depend on the real-space discretization in the longitudinal direction, the cutoff of the transverse momentum (see Ref. 5 for details), and the aspect ratio W/L. Extracting the conductivity using Eq. (4) is different from Ref. 5, where the conductivity was identified with LG/W. The advantage of Eq. (4) is that it eliminates the effect of an additive resistance from a region of ballistic transport adjacent to the contacts to the source and drain reservoirs and, hence, gives accurate conductivities for smaller sample sizes than the identification of σ and LG/W. Our procedure is illustrated in Fig. 1, where we show typical quantum numerical results for the resistance $R=1/G$ and the conductivity $\sigma(L)$ defined through Eq. (4).

We restrict the analysis of our numerical data to samples with length $L\gtrsim\ell$. (In semiclassical transport, this is the regime where electron motion is diffusive.) According to the Boltzmann theory, $\ell\sim\xi^3 n/K_0$. In the diffusive regime, the quantum conductivity σ has a weak dependence on the sample length L because of weak antilocalization. In order to

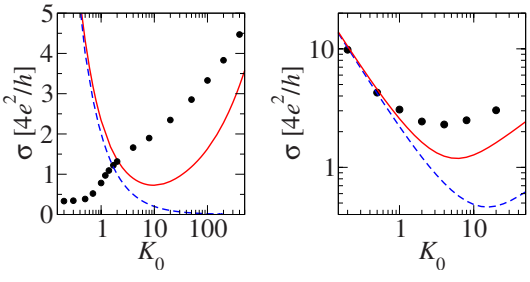

FIG. 3. (Color online) Conductivity σ versus disorder strength at the Dirac point (left) and at carrier density $\pi n=K_0/(\pi\xi)^2$, corresponding to the edge of the minimum conductivity plateau of Ref. 8 (right). Data points are from the numerical calculation for $L=50\xi$, and the (solid) dashed curves represent the (self-consistent) Boltzmann theory.

compare numerical data at different K_0 or n, we use two different procedures. In Figs. 2 and 3, we compare conductivities at a reference sample length $L=50\xi$, which is well inside the diffusive regime if $K_0 \gtrsim 1$. For this sample size and beyond, the L dependence of the conductivity was consistent with the theoretical expectation $d\sigma/d\ln L = 4e^2/\pi h$ of weak antilocalization theory for all carrier densities if $K_0 \gtrsim 1$. (Representative data for $K_0=2$ are shown in Fig. 1.) At the Dirac point, this size dependence of the conductivity was previously observed in Refs. 5, 7, and 15.

Figure 2 shows the conductivity $\sigma(L=50\xi)$ versus the carrier density n for two values of K_0. For $n\xi^2 \gtrsim 1$ the conductivity is well described by the asymptotic behavior of Eq. (2), the dominant correction term being proportional to $n^{1/2}$. Replacing the carrier density n by the self-consistent carrier density n^* (solid lines) further improves the agreement. For small densities, the quantum conductivity shows a sharp minimum at the Dirac point $n=0$, which is most pronounced for small disorder strengths. Such a dip is not present in either the Boltzmann theory or its self-consistent modification. Since in the quantum theory σ increases with increasing K_0 at the Dirac point but decreases with increasing K_0 away from the Dirac point, the quantum σ vs n curves of different K_0 cross somewhere in the region $0 < \pi n\xi^2 \lesssim 1$ for the parameter range we consider. This reversal in behavior was previously noted by Lewenkopf *et al.*[16] in numerical simulations of a tight-binding model, although the numerical data of Ref. 16 do not allow a conclusion to be made about large carrier density. The agreement at high carrier density between the quantum and the Boltzmann theory is an important new result of this work.

In Fig. 3, we address the conductivity as a function of disorder, comparing the quantum and Boltzmann theories. Motivated by prediction of Ref. 8 that the σ vs n curve exhibits a plateau of width $\sim K_0/\xi^2$ near the Dirac point, we consider the conductivity at the Dirac point $n=0$ (left panel) as well as near the edge of the proposed plateau, at $\pi n = K_0/(\pi\xi)^2$ (right panel).[17] The numerical calculations at the plateau edge are in good qualitative agreement with the self-consistent Boltzmann theory. At the Dirac point, however, σ is found to increase with K_0 for the entire parameter range we consider, which differs from the prediction of the Boltzmann theory[18] and the self-consistent Boltzmann theory. The former predicts $\sigma = 8e^2/K_0 h$ at the Dirac point, whereas the latter deviates from this prediction for $K_0 \sim 1$, reaches a minimum at $K_0 \approx 9.71$, and crosses over to the asymptotic dependence $\sigma \sim 2e^2 K_0^{1/2}/\pi h$ for $K_0 \gg 10$. At large K_0 the numerical data follow the trend of the self-consistent theory, although we cannot confirm the asymptotic dependence $\propto K_0^{1/2}$ from the parameter range studied in our simulations. Upon reducing K_0 below unity, the conductivity first decreases sharply, consistent with a renormalization of the mean-free path ℓ for $K_0 \lesssim 1$.[6,19] Upon reducing K_0 further, the Dirac point conductivity saturates at the ballistic value $\sigma = 4e^2/\pi h$.

The system-size-dependent weak antilocalization correction [Eq. (3)] is included in Figs. 2 and 3, which show σ at the reference length $L=50\xi$. In Fig. 4 we subtract the

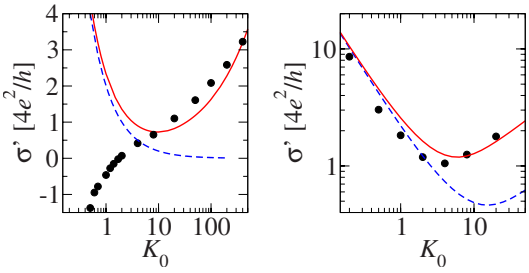

FIG. 4. (Color online) Same as Fig. 3 but for $\sigma' = \lim_{L\to\infty}[\sigma(L) - \pi^{-1}\ln(L/\xi)]$.

L-dependent logarithmic increase and show the K_0 dependence of $\sigma' = \lim_{L\to\infty}[\sigma(L) - \pi^{-1}\ln(L/\xi)]$.[20] Subtracting weak antilocalization significantly improves the agreement with the self-consistent theory at large K_0. Unlike the conductivity at the reference length $L=50\xi$, which saturates at $4e^2/\pi h$ for small K_0, σ' continues to decrease without bounds if K_0 is lowered.

The increase in σ with K_0 at the Dirac point for weak disorder is markedly different from the prediction of the Boltzmann theory. A key assumption of this theory and its self-consistent modification is that the graphene electron liquid can be mapped to an essentially homogeneous system with an effective carrier density n^* equal to the rms of a fluctuating "local" density determined by the random potential U. This assumption becomes questionable at the Dirac point, where the electron liquid is broken up in puddles of electronlike and holelike regions. At weak disorder, $K_0 \ll 1$, quantum fluctuations spread the carriers over many puddles and the concept of a local carrier density becomes problematic. It is in this regime that the difference between the quantum and Boltzmann calculations is, as expected, most pronounced.

The Gaussian random potential used here is the potential of choice for comparisons of analytical theories and numerical simulations. Yet, it differs in essential ways from the random potential in realistic graphene samples that do not have Gaussian statistics since it is likely caused by charged impurities in the substrate with a typical distance d from the graphene sheet smaller than the spacing between impurities. Still, it may be possible to extract equivalent parameters K_0 and ξ from a realistic random potential (see Ref. 11), implying that the sharp dip in conductivity predicted in the quantum theory would occur in a window of $n \sim 5\times 10^{10}$ cm^{-2} around the Dirac point.[21] This feature has not been observed in experiments.[10,22–24] Reasons why the dip has not been seen could be a suppression of quantum coherence by finite temperature effects or rippling[25] of the graphene sheet, or long-range fluctuations of the mean carrier density which effectively smear the feature near $n=0$.[26]

We thank C. Beenakker for comments on the manuscript. S.A. thanks the Aspen Center for Physics for its hospitality where some of this work was completed. This work is supported by the U.S. ONR, the NSF-NRI-SWAN, the Packard Foundation, and the NSF under Grant No. DMR 0705476.

[1] K. S. Novoselov, A. K. Geim, S. V. Morozov, D. Jiang, M. I. Katsnelson, I. V. Grigorieva, S. V. Dubonos, and A. A. Firsov, Nature (London) **438**, 197 (2005); Y. Zhang, Y.-W. Tan, H. L. Stormer, and P. Kim, *ibid.* **438**, 201 (2005).

[2] M. I. Katsnelson, K. S. Novoselov, and A. K. Geim, Nat. Phys. **2**, 620 (2006); K. Nomura and A. H. MacDonald, Phys. Rev. Lett. **98**, 076602 (2007); E. H. Hwang, S. Adam, and S. Das Sarma, *ibid.* **98**, 186806 (2007); J. Martin, N. Akerman, G. Ulbricht, T. Lohmann, J. H. Smet, K. von Klitzing, and A. Yacoby, Nat. Phys. **4**, 144 (2008); V. V. Cheianov, V. I. Falko, B. L. Altshuler, and I. L. Aleiner, Phys. Rev. Lett. **99**, 176801 (2007); E. Rossi and S. Das Sarma, *ibid.* **101**, 166803 (2008); I. Snyman, J. Tworzydlo, and C. W. J. Beenakker, Phys. Rev. B **78**, 045118 (2008).

[3] E. Fradkin, Phys. Rev. B **33**, 3257 (1986); A. W. W. Ludwig, M. P. A. Fisher, R. Shankar, and G. Grinstein, *ibid.* **50**, 7526 (1994); N. Shon and T. Ando, J. Phys. Soc. Jpn. **67**, 2421 (1998); M. I. Katsnelson, Eur. Phys. J. B **51**, 157 (2006); J. Tworzydlo, B. Trauzettel, M. Titov, A. Rycerz, and C. W. J. Beenakker, Phys. Rev. Lett. **96**, 246802 (2006).

[4] H. Suzuura and T. Ando, Phys. Rev. Lett. **89**, 266603 (2002).

[5] J. H. Bardarson, J. Tworzydlo, P. W. Brouwer, and C. W. J. Beenakker, Phys. Rev. Lett. **99**, 106801 (2007).

[6] A. Schuessler, P. M. Ostrovsky, I. V. Gornyi, and A. D. Mirlin, Phys. Rev. B **79**, 075405 (2009).

[7] J. Tworzydlo, C. W. Groth, and C. W. J. Beenakker, Phys. Rev. B **78**, 235438 (2008).

[8] S. Adam, E. H. Hwang, V. M. Galitski, and S. Das Sarma, Proc. Natl. Acad. Sci. U.S.A. **104**, 18392 (2007).

[9] Alternative models to Coulomb scattering have been examined by F. Schedin, A. K. Geim, S. V. Morozov, E. W. Hill, P. Blake, M. I. Katsnelson, and K. S. Novoselov, Nature Mater. **6**, 652 (2007) and L. A. Ponomarenko, R. Yang, T. M. Mohiuddin, M. I. Katsnelson, K. S. Novoselov, S. V. Morozov, A. A. Zhukov, F. Schedin, E. W. Hill, and A. K. Geim, Phys. Rev. Lett. **102**, 206603 (2009).

[10] Y.-W. Tan, Y. Zhang, K. Bolotin, Y. Zhao, S. Adam, E. H. Hwang, S. Das Sarma, H. L. Stormer, and P. Kim, Phys. Rev. Lett. **99**, 246803 (2007).

[11] S. Adam, S. Cho, M. S. Fuhrer, and S. Das Sarma, Phys. Rev. Lett. **101**, 046404 (2008).

[12] Quantum effects are a small correction to the conductivity only if the carrier density n is increased at fixed sample size L. This is the experimentally relevant limit. If the limit $L\to\infty$ is taken at fixed n, quantum effects dominate [see Eq. (3)]. We are therefore not considering the conceptually simple question of how quantum transport becomes classical as the phase coherence length decreases but the more interesting question of how this quantum-Boltzmann crossover depends on the carrier density and disorder strength.

[13] The Boltzmann conductivity differs from that of the self-consistent Born approximation (SCBA) if K_0 is not small. The origin of the discrepancy is the predominance of forward scattering if $n\xi^2 \gg 1$ and the breakdown of the noncrossing approximation in this case.

[14] For the theory of Ref. 8, where electron-electron interactions play a crucial role, the potential U is the screened disorder potential. The screened disorder potential depends on n^* so that one has to solve n^* self-consistently. For the unscreened version of the theory we consider here, such self-consistency is not required.

[15] K. Nomura, M. Koshino, and S. Ryu, Phys. Rev. Lett. **99**, 146806 (2007).

[16] C. H. Lewenkopf, E. R. Mucciolo, and A. H. Castro Neto, Phys. Rev. B **77**, 081410(R) (2008).

[17] We have also considered a model where we replace the random potential U with its absolute value $|U|$, which gives results similar to those on the right panel of Fig. 3.

[18] Kinetic equation approaches attempting to go beyond the Boltzmann theory, such as M. Auslender and M. I. Katsnelson, Phys. Rev. B **76**, 235425 (2007) and M. Trushin and J. Schliemann, Phys. Rev. Lett. **99**, 216602 (2007), behave qualitatively similar to the Boltzmann theory.

[19] I. L. Aleiner and K. B. Efetov, Phys. Rev. Lett. **97**, 236801 (2006).

[20] The data point at $K_0=0.5$ was obtained using extrapolation to large system sizes via the one-parameter scaling hypothesis (see Ref. 5).

[21] We also ignore screening, although, in principle, the effects of screening can be reduced significantly by using high-κ dielectrics (see Ref. 24 and references therein).

[22] K. S. Novoselov, A. K. Geim, S. V. Morozov, D. Jiang, Y. Zhang, S. V. Dubonos, I. V. Grigorieva, and A. A. Firsov, Science **306**, 666 (2004).

[23] J. H. Chen, C. Jang, S. Adam, M. S. Fuhrer, E. D. Williams, and M. Ishigami, Nat. Phys. **4**, 377 (2008).

[24] C. Jang, S. Adam, J. H. Chen, E. D. Williams, S. Das Sarma, and M. S. Fuhrer, Phys. Rev. Lett. **101**, 146805 (2008).

[25] S. V. Morozov, K. S. Novoselov, M. I. Katsnelson, F. Schedin, L. A. Ponomarenko, D. Jiang, and A. K. Geim, Phys. Rev. Lett. **97**, 016801 (2006).

[26] In this context, we note that the Gaussian model used here ignores the long-range tails in the Coulomb potential of charged impurities. See E. Rossi, S. Adam, and S. Das Sarma, arXiv:0809.1425 (unpublished).